Journal of Hydrology (2006) 330, 235–248

available at www.sciencedirect.com

ScienceDirect

journal homepage: www.elsevier.com/locate/jhydrol

Differential gauging and tracer tests resolve seepage fluxes in a strongly-losing stream

C. Ruehl [a,*], A.T. Fisher [a,b], C. Hatch [a], M. Los Huertos [c,d], G. Stemler [a], C. Shennan [c,d]

[a] *Earth Sciences Department, University of California, E&MS rm A232, 1156 High Street, Santa Cruz, CA 95064, USA*
[b] *Institute for Geophysics and Planetary Physics, University of California, 1156 High Street, Santa Cruz, CA 95064, USA*
[c] *Environmental Studies Department, University of California, 1156 High Street, Santa Cruz, CA 95064, USA*
[d] *Center for Agroecology and Sustainable Food Systems, University of California, 1156 High Street, Santa Cruz, CA 95064, USA*

Received 28 July 2005; received in revised form 24 March 2006; accepted 27 March 2006

KEYWORDS
Seepage;
Recharge;
Stream transport;
Tracers;
Water balance

Summary The Pajaro River, central coastal California, consistently loses 0.2–0.4 m^3/s of discharge along an 11.42-km experimental reach late in the water year, when discharge is $\leqslant$4.5 m^3/s. Channel loss occurs throughout this reach, but is greatest in magnitude near the bottom of the reach. Water isotopic data and other observations suggest that channel loss results mainly from streambed seepage, as opposed to evapotranspiration. If it occurs throughout the year, the channel loss along this short stream reach could contribute $6–13 \times 10^6$ m^3 of annual aquifer recharge, or ~20–40% of current sustainable basin yield. We performed a series of tracer injections along this reach to determine if hydrologic exchange occurs within this strongly-losing stream. We found that during periods of high channel loss, there were also comparable storage exchange fluxes and lateral inflow of tracer-free water. Within upper and lower parts of the experimental reach, storage exchange fluxes are about 10 times greater than lateral inflow. The former are associated with the movement of water between the main channel and surface or subsurface storage zones. In this system, it is likely that the latter are primarily associated with spatially- or temporally-long subsurface flow paths within the shallow streambed, as opposed to inflow of ground water from deeper in the basin. Along both upper and lower parts of the experimental reach, lateral inflow tends to increase as channel discharge decreases. In contrast, storage exchange fluxes increase with decreasing discharge along the upper parts of the reach, but decrease with decreasing discharge along the lower parts. Gauging and tracer test results suggest that subsurface storage exchange and loss may occur

* Corresponding author. Tel.: +1 831 459 1724.
E-mail address: cruehl@ucsc.edu (C. Ruehl).

0022-1694/$ - see front matter
doi:10.1016/j.jhydrol.2006.03.025

simultaneously, and that the lateral inflow of tracer-free water can be caused by long-scale subsurface flow as well as ground water making its first appearance in the channel.

Introduction

Surface water and ground water are increasingly viewed as a single resource within linked reservoirs (Jones and Mulholland, 2000; Winter et al., 1998). The movement of water from streams to aquifers and from aquifers to streams influences both the quantity and quality of available water within both reservoirs, depending on the magnitudes of fluxes, the initial chemistry of water moving through the stream bed, and transformations that occur during transport. These fluxes are driven by differences between stream water levels and hydraulic heads in the stream bed and aquifers adjacent to the stream channel. They occur over a range of time and length scales, and are influenced by channel geomorphology, lithologic variability, and hydrogeologic properties of the streambed and near-stream formations.

We use the term ''streambed seepage'' in this paper to refer to the movement of water across the streambed, both into and out of the stream channel. Where there is net loss in stream channel discharge due to streambed seepage, aquifer recharge may occur if the infiltrating water reaches the water table, or water may be used by riparian plants or remain in the vadose zone above the water table. Similarly there may be a net gain in channel discharge under baseflow conditions, when ground water moves into the stream. Alternatively, seepage may contribute to hyporheic flow, the movement of stream channel water into the shallow subsurface with subsequent return to the channel and no net change in channel discharge (Fig. 1). This definition of hyporheic flow, essentially process based, is a compromise of usage applied by ecologists, biologists, and hydrologists (Bencala et al., 1984; Bencala and Walters, 1983; Grimm and Fisher, 1984; Malard et al., 2002; Triska et al., 1989; Williams and Haynes, 1974).

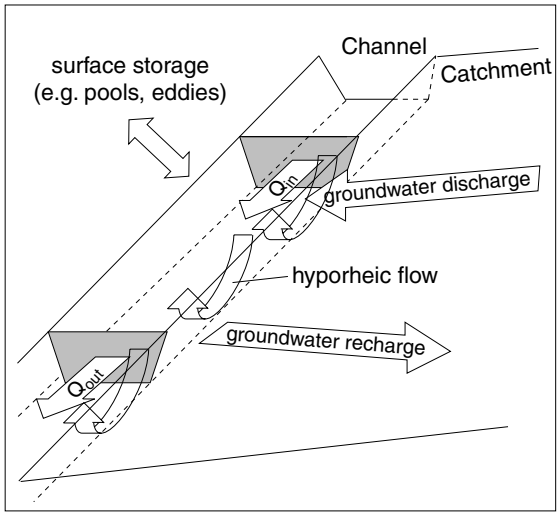

Figure 1 Cartoon showing surface–subsurface (seepage) exchange concepts (Harvey et al., 1996; Woessner, 2000). Channel discharge occurs at the upper and lower ends of an experimental reach. Tracer is injected at the upper end of the reach and monitored as the lower end of the reach. During transport down the reach, water exchanges with storage areas in and off the channel, above and below the stream bottom.

Thus streambed seepage comprises both lateral inflow and outflow of ground water and hyporheic exchange, including all subsurface flow paths that start and end at the streambed (Fig. 1). One of the major goals of this study was to estimate the magnitude of the seepage flux within a specific stream system, as well as the contributions of its components (the hyporheic flux, inflow of ground water, and outflow of ground water). The extent of seepage across streambeds has been linked to various characteristics of previously studied stream systems, including parent lithology (Valett et al., 1996), variations in stream gradient (Harvey and Bencala, 1993; Hill et al., 1998; Wondzell and Swanson, 1996), and formation and migration of sediment bedforms (Packman and Brooks, 2001). Several recent studies have documented aquifer recharge contributions made by streams using field observations, geochemical data, and modeling (Criss and Davidson, 1996; Izbicki et al., 2004; Rains and Mount, 2002). Water management goals towards sustainable ground water extraction often include maintenance of stream discharges sufficient to support aquatic ecologic systems, which requires knowledge of seepage rates both into and out of the streambed.

The most commonly used method for evaluating subsurface–surface exchange at long spatial scales (i.e., greater than ~100 m) is use of transient storage models (TSMs) (Harvey and Wagner, 2000). One important limitation of the TSM approach is that multiple (complex) surface and subsurface storage zones are combined into a single (highly idealized) storage zone (Choi et al., 2000). In addition, many applications of TSMs assume that the frequency distribution of storage zone residence times is exponential, whereas non-exponential residence time distributions are more consistent with experiment in some systems (Gooseff et al., 2003b; Haggerty et al., 2002; Worman et al., 2002). Also, storage exchange that occurs over time or length scales longer than that of the tracer test may not be properly represented (Harvey et al., 1996; Zaramella et al., 2003); most stream tracer studies last several hours to a few days, but longer-scale (temporal, spatial) exchange is important in some systems (Gooseff et al., 2003a; Haggerty et al., 2002; Kasahara and Wondzell, 2003; Storey et al., 2003). Nevertheless, the TSM approach remains useful for quantitative (albeit highly idealized) characterization and comparison of stream systems (Gooseff et al., 2005; Harvey et al., 1996; Wagner and Harvey, 1997). In this study, we apply a TSM approach in combination with a detailed water budget in an attempt to estimate both short and long-scale hyporheic flow. Although subsurface–surface exchange at a wide range of time and length scales has been observed in many streams, few studies compared inflow and

outflow fluxes of ground water, and hyporheic exchange, at multiple spatial scales.

We have completed a study of streambed seepage and related biogeochemical processes within a strongly-losing stream that supplies a large portion of basin-wide aquifer recharge. Most previous work on hyporheic flow in streams has focused on discharge-neutral or gaining streams (Bencala, 1983; Fernald et al., 2001; Haggerty et al., 2002; McKnight et al., 2002), although a smaller number of studies have provided evidence of hyporheic flow in losing reaches of streams (e.g., Harvey and Fuller, 1998). In this paper we use differential gauging and tracer tests to examine adjacent losing and non-losing parts of a stream, quantify rates of streambed seepage, and assess how conceptual models of seepage processes and quantitative methods can be applied to a losing stream. We explore how seepage fluxes change during the water year, with variations in channel discharge. In particular, we test the hypothesis that seepage fluxes relative to discharge increase as discharge decreases. This work also helps to assess how much aquifer recharge occurs via streambed seepage, or might occur through management of stream flows, within an overdrafted coastal basin. The hydrologic results obtained in this study are also essential to a thorough analysis of water quality, particularly of elevated nitrate concentrations, in this stream system (Ruehl et al., 2006).

Field and experimental setting

Geology, climate, and hydrology

The Pajaro River is a fourth-order stream that drains a 3394 km^2 basin in central coastal California (Fig. 2) (Hanson, 2003). The basin is bounded by the Santa Cruz Mountains on the northwest, the Gabilan Range on the southwest, and the Diablo Range on the east. The San Andreas Fault Zone, which trends northwest to southeast as it crosses the basin, intersects the Pajaro River at Pajaro Gap. Southwest of this fault system, the Pajaro Valley is underlain primarily by late Tertiary strata and Cretaceous granodiorite basement (Greene, 1990). The Tertiary strata consist primarily of alluvial Holocene deposits, the Aromas Formation (Pleistocene), and the Purisima Formation (Pliocene). In the Pajaro Valley, these deposits have a maximum thickness of 1200 m (Muir, 1972). In contrast, the parent lithologies northeast of the fault are primarily marine sedimentary rocks of late Mesozoic and early Tertiary age. These units have relatively low hydraulic conductivities, and thus the San Andreas Fault Zone is considered to be the eastern boundary of the Pajaro Valley ground water basin (Muir, 1972).

Mean daily discharge recorded at the US Geological Survey (USGS) gauging station at the top of the experimental reach (Station #11159000) was between 0 and 610 m^3/s from 1939 to 2003. Average daily high temperatures in nearby Watsonville are 16 °C to 23 °C, and average lows are 3 °C to 12 °C. Average annual precipitation is 33 cm in Hollister (Santa Clara Valley, the eastern part of the Pajaro River basin) and 55 cm in Watsonville (Pajaro Valley, the western part of the basin). Typically over 90% of annual precipitation occurs from October to May, and by late summer (August and September) no significant precipitation has fallen for four to five months. This precipitation pattern results in normal stream discharges ranging from 1 to 250 m^3/s during the rainy season and from 0 to 0.5 m^3/s during the dry season (Fig. 3).

Ground water is the primary water source for irrigation in the basin (in which agriculture is the dominant land

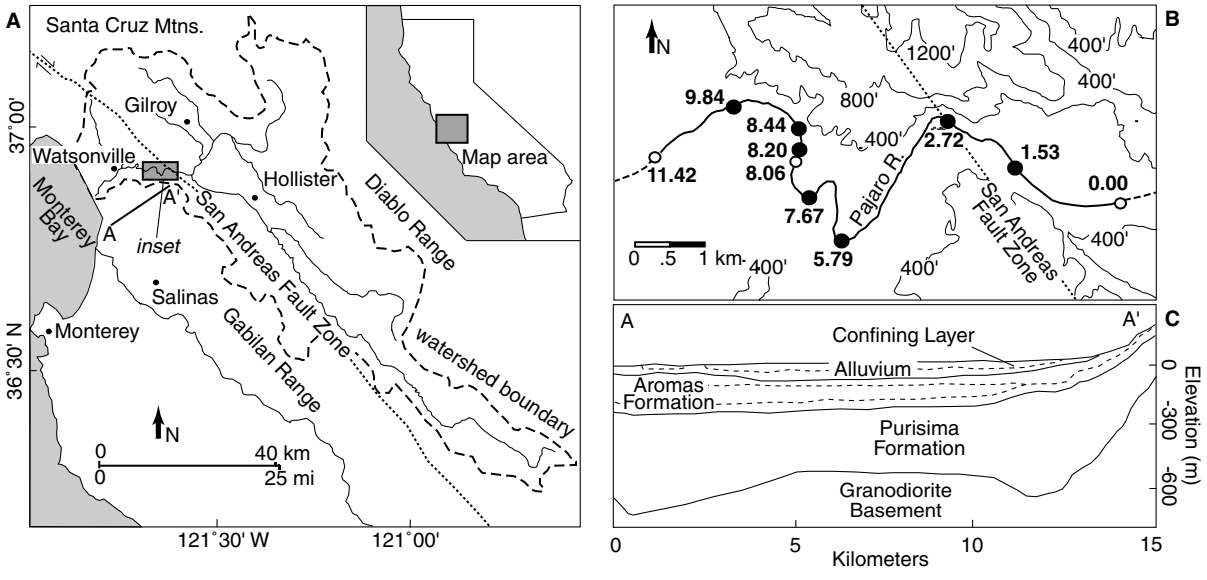

Figure 2 Maps of the field site. (A) The Pajaro River watershed, along the central coast of California. Shown are the locations of the inset map (B) and the geologic cross-section (C). (B) The 11.42-km experimental reach of the Pajaro River. All sites (in boldface) are identified by distance (in km) downstream from the top of the reach, site of a USGS gauging station. Continuous discharge records are presented for sites marked with open circles. (C) Shallow stratigraphy of the Pajaro Valley along transect A—A′ (including the experimental reach), with the major water-bearing formations (the Alluvium, the Aromas, and the Purisima). Modified from Hanson (2003).

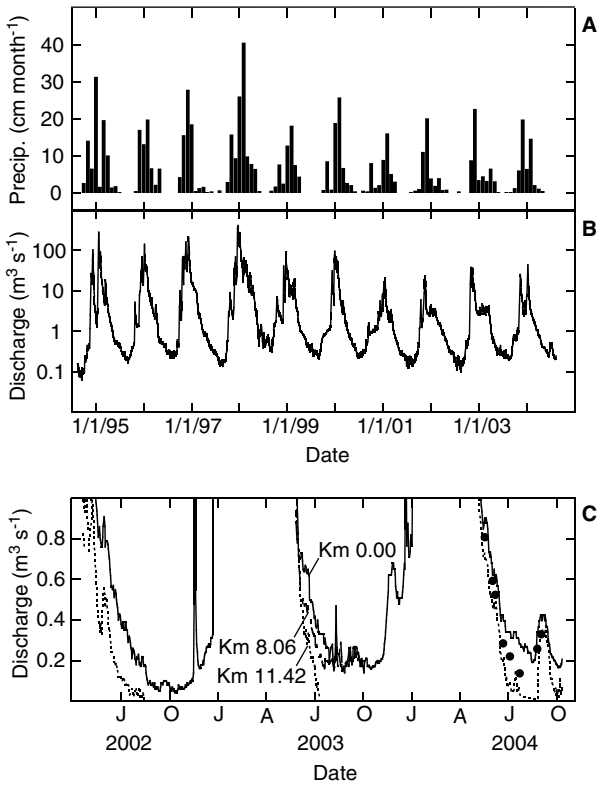

Figure 3 Precipitation and discharge along the Pajaro River, central coastal California, USA. (A) Ten-year record of monthly precipitation recorded in the Watsonville, adjacent to the experimental reach. (B) Ten-year record of mean daily stream discharge at the Chittenden USGS gauging station (Km 0.00). (C) Three-year record of stream discharge at Km 0.00 (solid line), Km 8.06 (dot-dashed line and closed circles), and Km 11.42 (dotted line).

use), and is extracted mainly from the alluvial and underlying Aromas aquifers (Muir, 1977; PVWMA, 2001). The current rate of ground water extraction in the basin is $\sim 8.5 \times 10^7$ m^3/year, which is $\sim 5.5 \times 10^7$ m^3/year greater than the estimated basin sustainable yield given current pumping patterns. This overdraft has resulted in both seawater intrusion near the coast and lowering of water levels in wells throughout the basin, with an estimated annual loss of $\sim 1.1 \times 10^7$ m^3 of freshwater storage (PVWMA, 2001). These values have large uncertainties, particularly because of difficulties in quantifying aquifer recharge, but there is no doubt that the Pajaro Valley ground water basin is seriously out of hydrologic balance. As in many coastal basins, population and water demand are expected to increase in coming years, and there is keen interest in quantifying streambed seepage rates and in understanding the properties and processes that control these rates.

Experimental design

Our study site is an 11.42 km reach of the Pajaro River, beginning with a USGS gauging station at Chittenden Road and ending at Murphy Road (Fig. 2B). All river distances reported within the experimental reach are downstream from the Chittenden gauging station. We refer to subsections of the experimental reach as ''stretches''. The river is constricted by local topography near Km 3 as it flows through Pajaro Gap, and near Km 9 as it flows through Chittenden Pass. The stream gradient over the entire reach is approximately 0.1%, with greater typical stream velocities in the upstream part of the reach and lower velocities as the Pajaro Valley widens downstream. During the spring, summer, and early fall, discharge generally decreases downstream along the reach. The stretch downstream from ~Km 9 typically goes dry by late summer and remains dry until after the first significant precipitation of the subsequent water year.

Throughout the study we concentrated sampling, measurements, and experiments on the second half of the water year (April–September) for several reasons. First, in order to evaluate the extent of stream seepage losses and gains, we need to constrain all other source and sink terms. There tends to be little precipitation during the second half of the water year, water is input only at the top of the experimental reach, the local water table is drawn below the level of the stream, and there is little or no hillslope runoff or net ground water input to the stream channel (as will be shown), all of which help to simplify mass balance calculations. Second, we wish to quantify as accurately as possible differences in stream discharge along the reach, determined by gauging, and this is easiest, safest, and most accurately done in the Pajaro River when discharge is below ~5 m^3/s. The velocity–area method used to assess stream discharge is generally accurate to ±5–10% (Rantz, 1982; Sauer and Meyer, 1992), and errors associated with rating curves and differential flow measurements at greater discharges could swamp typical differences in channel discharge on the order of 0.2–0.4 m^3/s.

Methods

Stream gauging

We obtained a time series (15-min sampling interval) of discharge entering the experimental reach (Q_{in}) from the USGS gauging station at Km 0.00 (Fig. 2B). This gauging system measures water depth with a gas bubbler and depth is converted to discharge with a rating curve based on field measurements made every 2–4 weeks. We installed additional pressure gauges at two other sites, Km 8.06 (water year 2003) and Km 11.42 (water years 2002–2004). These gauges consist of pressure transducers installed in stilling wells (nominal 4 mm resolution) with electronic data logging at 15-min intervals. We calibrated these transducers in the field, and monitored drift relative to a staff plate at monthly intervals. We developed rating curves for the stations at Km 8.06 and Km 11.42, and checked the rating curve developed by the USGS at Km 0.00, with repeated velocity–area surveys at each site. We determined volumetric discharge values using a pygmy-Price flow meter and standard methods (Rantz, 1982). In addition to measuring discharge at sites where continuous gauges were installed, we also performed periodic ''seepage runs'', where discharge was

measured at 2–4 locations along the experimental reach during a single day, to determine where channel loss occurred most rapidly. We made stream velocity measurements at 6/10 water depth, and spaced these measurements laterally to ensure that no more than 5% of the total stream discharge occurred between any two measurements (typically 20–60 cm apart). Interpretation of discharge data and planning for tracer experiments were aided with regional precipitation and evaporation data collected by the California Irrigation Management Information System (CIMIS; http://www.cimis.water.ca.gov), which includes several stations in the Pajaro Valley and surrounding area.

Water isotope analyses

We obtained water samples for isotopic analyses at several sites along the experimental reach from surface, streambed, and ground water reservoirs. Samples were collected in pre-cleaned amber glass bottles after the bottles were rinsed three times with water, and then capped with ''sure-seal'' lids to prevent evaporative loss. Samples were shipped to the Center for Stable Isotope Biogeochemistry at the University of California, Berkeley and analyzed on a dual-inlet mass spectrometer. External standards were run after every six field samples. Based on these standards, we determined that the stable isotope ratios obtained for water were accurate to within 0.13‰ for $\delta^{18}O$ and 0.50‰ for $\delta^{2}H$.

Tracer tests

Field and lab procedures

During the summers of 2003 and 2004 we conducted twelve tracer tests in the Pajaro River, along stretches 650–3370 m long (Table 1). We measured discharge with the velocity area method to determine flow into (Q_{in}) and out of (Q_{out}) each experimental stretch, often as part of a longer seepage run along a part of the complete reach. For five of the tests, a 1% Rhodamine-WT (RhWT) solution was injected at a constant rate for 4–6 h. For the other seven tests, a solution containing both RhWT and sodium bromide (NaBr, 400 g/L) was injected at a constant rate for 4–6 h. During injectate preparation, we measured total tracer masses to be injected, and during injections we closely monitored injection rates and durations. At observation sites upstream and downstream from the injection sites, we collected samples and stored them unfiltered in amber glass bottles placed in a closed box. Samples were collected manually at 5–15 min intervals during and for several hours after the end of injection, and automated samplers were used to collect additional samples at longer time intervals for 12–36 h following injection for most tests. We recovered samples collected automatically from the field within 12–18 h of collection, and glass bottles were used in the automated samplers to minimize RhWT adsorption. We also collected two or more samples from the stream by hand at the same time as the automated samplers during each deployment; in all cases, tracer concentrations determined

Table 1 Summary of tracer tests

Date	Injection (river Km)	Length (m)	Q_{in} (m^3/s)	Q_{out} (m^3/s)	$F_{D,RhWT}$ (−)	$F_{D,Br}$ (−)
8/26/03	7.67	770	0.099	0.058	1.12	1.08
8/28/03	5.79	930	0.22	0.19	1.09	N/A[a]
		950	0.19	0.12	1.19	N/A
9/2/03	2.72	3070	0.19	0.16	1.14	N/A
9/4/03	0.00	1530	0.20	0.20	1.20	N/A
		1190	0.20	0.19	1.03	N/A
5/17/04	5.79	1880	0.66	0.58	1.05	N/A
		3730	0.58	0.49	1.19	N/A
5/19/04	0.00	2720	0.67	0.66	1.10	N/A
		3070	0.66	0.61	1.33	N/A
6/15/04	7.67	770	0.26	0.26	1.15	1.08
6/17/04	0.00	2720	0.32	0.29	1.27	1.11
7/20/04	7.67	650	0.13	0.11	1.18	1.09
7/22/04	0.00	1530	0.21	0.21	1.19	1.10
		1190	0.21	0.21	1.10	1.09
8/31/04	7.67	770	0.28	0.27	1.14	1.11
9/2/04	0.00	1530	0.37	0.38	1.10	1.09
		1190	0.38	0.33	1.04	1.02

[a] Not applicable (Br^- was not injected).

from samples collected by hand and with the automated samplers agreed within instrumental precision. We collected background samples upstream from each injection site throughout the experiments; these samples were stored, transported, and analyzed following procedures identical to those used for downstream samples. All samples equilibrated thermally and settled overnight in the laboratory prior to analysis to avoid interference with RhWT (fluorometric) analysis (Wilson et al., 1986).

We measured RhWT concentrations in the field periodically during the tests with a Turner 8000 fluorometer, to guide experimental procedures, and all samples were analyzed later in the lab to obtain more quantitative results. Blank and reference standards were run every ten samples. We pipetted subsamples (0.45 μm pore size) and determined Br concentrations with a Dionex DX-100 ion chromatograph. Replicate measurements of three complete BTCs from different tests produced standard deviations $\leqslant$0.5 μg/L for RhWT and $\leqslant$0.05 mg/L for Br. The different methods used for analysis of RhWT and Br concentrations avoid interference effects resulting from co-injection (Jones and Jung, 1990).

Interpretation of breakthrough curves

We interpret experimental tracer breakthrough curves (BTCs) to quantify seepage fluxes using several approaches. We first calculate a tracer dilution factor (F_D) as:

$$F_D = \frac{m_{inj}}{Q_{in} \int C\,dt} \tag{1}$$

where Q_{in} (m^3/s) is the discharge at the upper endpoint of the stretch (injection point), C is the channel tracer concentration in excess of background concentration, and m_{inj} is the total mass of injected tracer. Apparent tracer dilution (i.e., $F_D > 1$) can be caused by non-conservative tracer behavior such as photodecay, or by the flow of tracer-free water into the main channel (either ''true'' ground water making its first appearance in the channel, or the return of hyporheic flow that originally entered the subsurface upstream of the tracer injection or before the injection began and thus contains no tracer). We note that use of the dilution factor is independent of the equations used to model BTCs, as discussed below; F_D depends only on the measured channel discharge, the area under the BTC, and the tracer mass injected, all of which are relatively easy to measure.

We also fit BTCs to results obtained with a one-dimensional model of advection, dispersion, and storage exchange (Bencala and Walters, 1983). Storage zones in these transient storage models (TSMs) are typically thought to comprise two physical components of the stream and riparian system: (1) in-channel and off-channel pools and eddies; (2) streambed and aquifer areas adjacent to the main channel that experience hyporheic flow (Fig. 1). For a conservative tracer experiencing an exponential distribution of storage residence times (Runkel, 1998):

$$\frac{\partial C}{\partial t} = -\frac{Q}{A}\frac{\partial C}{\partial x} + \frac{1}{A}\frac{\partial}{\partial x}\left(AD\frac{\partial C}{\partial x}\right) + \frac{q_{L,in}}{A}(C_L - C) + \alpha(C_S - C) \tag{2}$$

$$\frac{\partial C_S}{\partial t} = -\alpha\frac{A}{A_S}(C_S - C) \tag{3}$$

where t is time, Q is main channel discharge, A is the main channel cross-sectional area, x is downstream distance, D is the dispersion coefficient, $q_{L,in}$ is lateral inflow of tracer-free water, C_L is the lateral inflow solute concentration, α is the main channel/storage zone exchange time constant, C_S is the storage zone solute concentration, and A_S is the storage zone cross-sectional area. As discussed later, we explored use of TSMs incorporating non-exponential residence time distributions to model tracer response in the Pajaro River, but found no improvement in fitting of data to understand hydrologic exchange.

Although the standard TSM equations are written in terms of a single value for stream discharge (Q), the code commonly applied to TSMs (OTIS) is capable of handling changes in stream discharge (Runkel, 1998; Runkel et al., 1998). Also, a ground water outflow term ($q_{L,out}$) is accounted for in OTIS and is estimated by simultaneously considering differential discharge data and dilution of injected tracers (Harvey and Wagner, 2000). This quantity is related to $q_{L,in}$, the net change in channel discharge, and the length of the stretch:

$$q_{L,out} = q_{L,in} - \frac{\Delta Q}{L} \tag{4}$$

Thus if Q remains constant throughout the reach, $q_{L,out} = q_{L,in}$ (both terms may be zero or non-zero). Similarly, if $Q_{out} < Q_{in}$, then $q_{L\text{-}out} > q_{L\text{-}in}$. As a practical matter, $q_{L,in}$ may include actual ground water flow to the stream and hyporheic flow that entered the streambed upstream from the injection point and leaves the streambed upstream from the sampling point. Similarly, $q_{L\text{-}out}$ may include water that leaves the stream channel permanently (enters an underlying aquifer or vadose zone) or hyporheic flow that bypasses the downstream sampling point (Harvey and Bencala, 1993). Transient storage parameters (D, A, A_s, α, and $q_{L,in}$) were estimated by non-linear optimization of models based on Eqs. (2) and (3) (Runkel, 1998) using a general parameter estimation code (PEST) (Doherty, 2004; Vecchia and Cooley, 1987). For each experiment and modeling effort, the goal was to minimize the sum of the squares of the residuals corresponding to each concentration observation, $\sum R = \sum (C_i^{obs} - C_i^{calc})^2$, where C_i^{obs} is the observed (normalized) tracer concentration at some time after start of injection, and C_i^{calc} is the modeled (normalized) tracer at the same time. Fit statistics for each tracer experiment and best-fitting model are summarized as composite residual magnitude $\phi = (\sum R/n)^{1/2}$, where n is the number of observations fit to model output.

Values of $q_{L,out}$ were determined on the basis of calculated values of $q_{L,in}$ and measured discharge at the top and bottom of each experimental stretch using Eq. (4). Once a best fit was achieved by optimization, a characteristic lateral inflow length (L_l) was calculated for each tracer experiment:

$$L_l = \frac{\overline{Q}}{q_{L,in}} \tag{5}$$

where $\overline{Q} = (Q_{in} + Q_{out})/2$ is the stretch-averaged discharge. We also calculated a characteristic storage zone exchange length (L_S) (Harvey and Bencala, 1993):

$$L_S = \frac{\overline{Q}}{\alpha \times A} = \frac{u}{\alpha} \tag{6}$$

where u is mean channel velocity at the stretch midpoint. We calculated a channel loss length (L_L) having similar units:

$$L_L = \frac{L \times \overline{Q}}{Q_{in} - Q_{out}} \quad (7)$$

Given a constant rate of channel loss, L_L represents the downstream distance from the stretch midpoint at which channel discharge would decrease to zero. To minimize the impact of errors in differential gauging, L_L was always calculated for total stretch lengths of >2 km. Collectively, these metrics are useful for comparing the magnitudes of net channel losses to storage and ground water exchange. We also calculated Dahmkohler numbers (DaI) associated with each tracer experiment to assess the likely reliability of estimated hydrologic parameters (Bahr and Rubin, 1987):

$$DaI = \frac{\alpha(1 + A/A_S)L}{u} \quad (8)$$

Different parameters are more sensitive to different parts of the BTC, but parameter estimates are generally most reliable for $0.1 \leqslant DaI \leqslant 10$ (Wagner and Harvey, 1997).

Results

Stream discharge and loss

Channel discharge measured along the experimental reach ranged from 0.15 m^3/s to 4.5 m^3/s. Calculated discharges falling above this range, based on extrapolation of rating curves, are subject to considerable error and were not used in subsequent analyses. During the three-year study period, mean daily discharges entering the reach exceeded 4.5 m^3/s on 10% of all days; however none of these days was later in the water year than March 16. In general, discharge decreased throughout the summer at all sites, although in mid-August 2004, a reservoir release upstream of the experimental reach caused discharge at Km 0 to increase abruptly from ~0.2 to ~0.4 m^3/s for approximately two weeks (Fig. 3C).

Comparison of discharge values at the different stations confirmed that there tended to be greater channel discharge at Km 0 than at Km 11.42. Discharge loss between these stations ranged from 0.2 to 0.4 m^3/s (Fig. 3C), equivalent to channel loss per unit stream length ($\Delta Q/L$) of 0.2–0.4 cm^2/s. The Pajaro River went dry at Km 11.42 in August of 2002 and 2003, but water continued to flow at Km 8.06 during both years. Throughout August and September 2003 there was no significant discharge loss from Km 0 to Km 8.06 (i.e., discharge loss greater than the 5% error expected for direct discharge measurements); the channel was completely dry at Km 11.42 during this time, indicating that channel loss on the lower ~3 km of the experimental reach occurred at ~1 cm^2/s. During the upstream (reservoir) release in August 2004, discharge increased abruptly at Km 11.42 to ~0.35 m^3/s and channel loss stopped temporarily. Channel loss resumed in September 2004, ~3 weeks after the release.

In addition to data collected continuously at 2–3 gauging stations along the experimental reach, discharge was measured at various places during 19 seepage runs between 7/7/03 and 9/8/04. In almost cases, discharge either remained constant (within measurement resolution) or decreased in the downstream direction (Fig. 4). These seepage runs support the interpretation that channel loss was

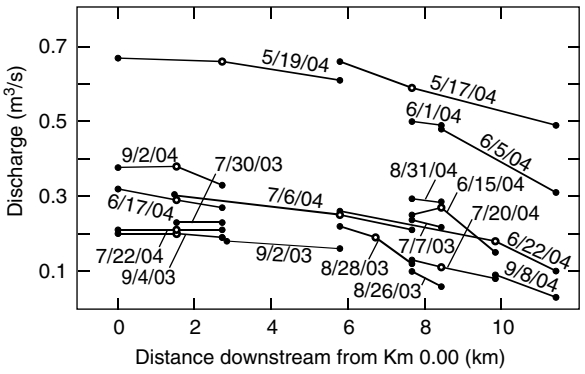

Figure 4 Results from 19 seepage runs along the experimental reach, during which discharge was measured at two or more sites on the same day. Closed circles represent the beginning or end of a seepage run, open circles represent a midpoint (when applicable).

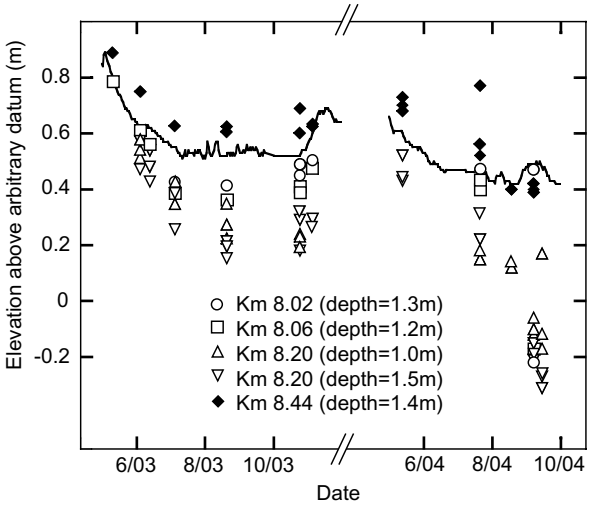

Figure 5 River stage and hydraulic head measured in piezometers along the lower stretch, both relative to the same arbitrary datum. Each of the five transects includes piezometers on the left, center, and right side of the channel.

less significant in the upper part of the reach, particularly in the stretch from Km 0 to Km 1.53, but was more significant in the lower part of the reach, including the stretch from Km 7.67 to Km 8.44. Water levels in transects of piezometers installed in the streambed along this lower portion of the reach (Km 8.02–8.20) were typically 0.1–0.3 m lower than in the main channel, equivalent to head gradients of ~10–30% directed into the streambed (Fig. 5). Interestingly, water levels in piezometers at Km 8.44 were often higher than those in the main channel, even months after significant precipitation had fallen.

Water isotope analyses

Stable water isotope ratios of samples collected in 2003 along the experimental reach of the Pajaro River show several notable features (Fig. 6). Data from surface and subsurface samples collectively indicate a crude trend that falls

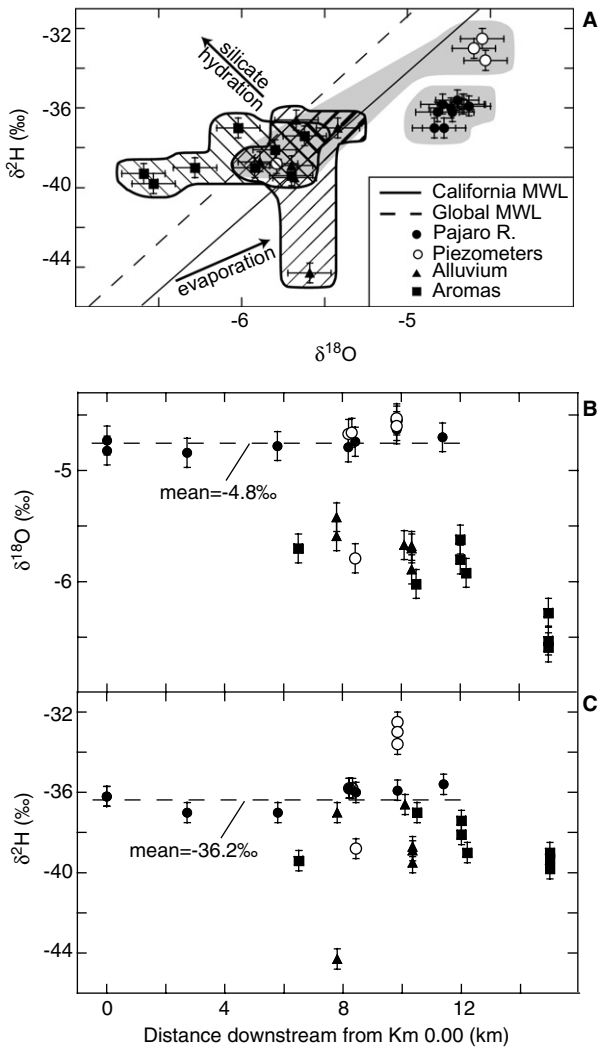

Figure 6 Stable isotope ratios ($\delta^{18}O$ and $\delta^{2}H$) of water in samples collected in 2003 from the Pajaro River, shallow streambed piezometers (screened <2 m below the streambed), and nearby ground water wells. Ground water wells are from the following aquifers: alluvial (screened 5–30 m below ground surface, mbgs), Upper Aromas (30–100 mbgs), and Lower Aromas (>100 mbgs). (A) $\delta^{2}H$ vs. $\delta^{18}O$ for all samples, along with the Global Meteoric Water Line and a MWL constructed for California (Kendall and Coplen, 2001).(B) $\delta^{18}O$ vs. river Km, with wells plotted at the nearest channel location. The mean value for river samples is indicated. (C) Same as B, but for $\delta^{2}H$.

across both global and regional meteoric mixing lines (Kendall and Coplen, 2001) (Fig. 6A). Pajaro River water was generally more enriched in both ^{2}H and ^{18}O in comparison to subsurface water, except for one set of streambed piezometer samples that was exceptionally enriched in ^{2}H. More significantly, Pajaro River water data cluster within a narrow range of $\delta^{2}H$ and $\delta^{18}O$, providing little evidence of evaporation during transport downstream. This last trend is also apparent in plots of $\delta^{2}H$ and $\delta^{18}O$ vs. downstream distance (Fig. 6B and C). Pajaro River water samples showed consistent mean values, $\delta^{18}O = -4.8‰ \pm 0.1‰$ and $\delta^{2}H = -36.2‰ \pm 0.5‰$. Samples collected from streambed piezometers and adjacent ground water wells were consistently less enriched in ^{18}O (Fig. 6B), and all ground water samples also had more negative $\delta^{2}H$ values (Fig. 6C). Additional surface water samples collected and analyzed in 2004 (data not shown) indicated greater seasonal variation in stable isotopic content, but the same lack of downstream trends as 2003 samples.

Tracer tests

We performed five RhWT injections and seven RhWT/NaBr co-injections along the experimental reach during the 2003 and 2004 water years. Bromide usually behaves conservatively in hydrologic systems (Levy and Chambers, 1987), whereas RhWT may be lost in some systems due to photodecay or adsorption (Shiau et al., 1993; Smart and Laidlaw, 1977; Sutton et al., 2001). For the nine Pajaro River stretches tested during the co-injections, the average dilution factor for RhWT was $F_{D,RhWT} = 1.14 \pm 0.07$, whereas that for Br was $F_{D,Br} = 1.08 \pm 0.03$ (Table 1). Minimum F_D values for RhWT and Br were 1.03 and 1.02, respectively, and the largest F_D value (1.33) was obtained for RhWT in the longest stretch tested (>3 km), when Br was not co-injected. The mean difference in F_D values when RhWT and NaBr were co-injected was 5%; in only one case was the difference greater than 10% (Table 1). Because F_D values were so similar, we conclude that RhWT behaved only slightly less conservatively than Br, and no corrections were applied to RhWT data. Tracer tests using both tracers were modeled using equations for conservative tracers.

Although hydrologic parameters along the entire experimental reach were quantified, we focus on two stretches with distinct characteristic responses during tracer experiments: Km 0.00–1.53 (''upper stretch'', five injections; Table 2), and from Km 7.67 to 8.44 (''lower stretch'', four injections; Table 3). We compare RhWT data and resulting models for all tests on the upper stretch, because not all injections on this stretch included Br (Table 1), whereas Br data are used for all tests and models on the lower stretch. The battery failed on the automated sampler deployed at Km 1.53 during one of the upper stretch injections (6/17/04). We obtained a BTC at Km 2.72 from this test, but sampling was stopped at this site when tracer concentrations were still ~10% above background levels relative to peak concentrations. We therefore could not calculate tracer recovery or a dilution factor for this test, although we were able to fit the model to the BTC. The Dahmkohler number for this experiment was 204, suggesting that the reach length was too long to allow for estimation of hydrologic exchange parameters with confidence (Wagner and Harvey, 1997), so results from this test are not used in subsequent analyses.

The TSM fit the data well for all upper stretch injections, during which channel discharge entering the stretch was 0.20–0.67 m^3/s (Fig. 7). The composite residual magnitude (ϕ) ranged from 1.0% to 2.1% for all tests with DaI numbers of 9–15 (Table 2). Best-fitting values of D, A, A_s, and α are broadly consistent with values estimated from other stream systems experiencing similar channel discharge (Bencala et al., 1990; D'Angelo et al., 1993). The TSM did not fit observed tracer data from the lower stretch as well as the upper stretch (ϕ = 2.8–5.1%), particularly when channel

Table 2 TSM parameters for Km 0.00 RhWT injections

Date	Q_{in} (m^3/s)	L (m)	D (m/s^2)	A (m^2)	A_s (m^2)	α (1/h)	ϕ (%)	Dal (−)	$q_{L,in}$ (cm^2/s)	A_s/A (−)	L_I (km)	L_S (km)	L_L (km)
9/4/03	0.20	1530	0.47	1.60	0.36	0.54	1.0	10.8	0.26	0.23	7.7	0.77	53
7/22/04	0.21	1530	0.68	2.47	0.50	0.47	1.2	13.8	0.26	0.20	8.1	0.66	N/A[b]
6/17/04	0.32	2720	0.43	2.81	2.84	16	N/C[a]	204	0.32	N/C	10	N/C	28
9/2/04	0.37	1530	0.54	2.89	0.54	0.43	1.2	9.1	0.24	0.19	15	1.1	24
5/19/04	0.67	2720	0.38	3.59	0.73	0.65	2.1	15.1	0.25	0.20	27	1.1	N/A

Length scales: L_I — lateral inflow; L_S — transient storage exchange; L_L — discharge loss.
[a] Not calculated, because Dal $\gg$ 10.
[b] Not applicable, because discharge did not decrease downstream.

Table 3 TSM parameters for Km 7.67 Br^- injections

Date	Q_{in} (m^3/s)	L (m)	D (m/s^2)	A (m^2)	A_s (m^2)	α (1/h)	ϕ (%)	Dal (−)	$q_{L,in}$ (cm^2/s)	A_s/A (−)	L_I (km)	L_S (km)	L_L (km)
8/26/03	0.099	530	0.43	2.35	0.87	0.026	5.1	0.45	0.14	0.37	5.2	4.6	1.5
7/20/04	0.13	650	0.33	3.04	0.57	0.11	3.4	2.9	0.18	0.19	6.7	1.3	4.6
8/31/04	0.28	770	0.13	2.71	1.20	1.1	2.8	7.4	0.40	0.44	6.9	0.33	21
6/15/04	0.67	770	0.64	3.52	0.71	0.19	3.8	3.4	0.70	0.20	9.6	1.4	4.3

Length scales: L_I — lateral inflow; L_S — transient storage exchange; L_L — discharge loss.

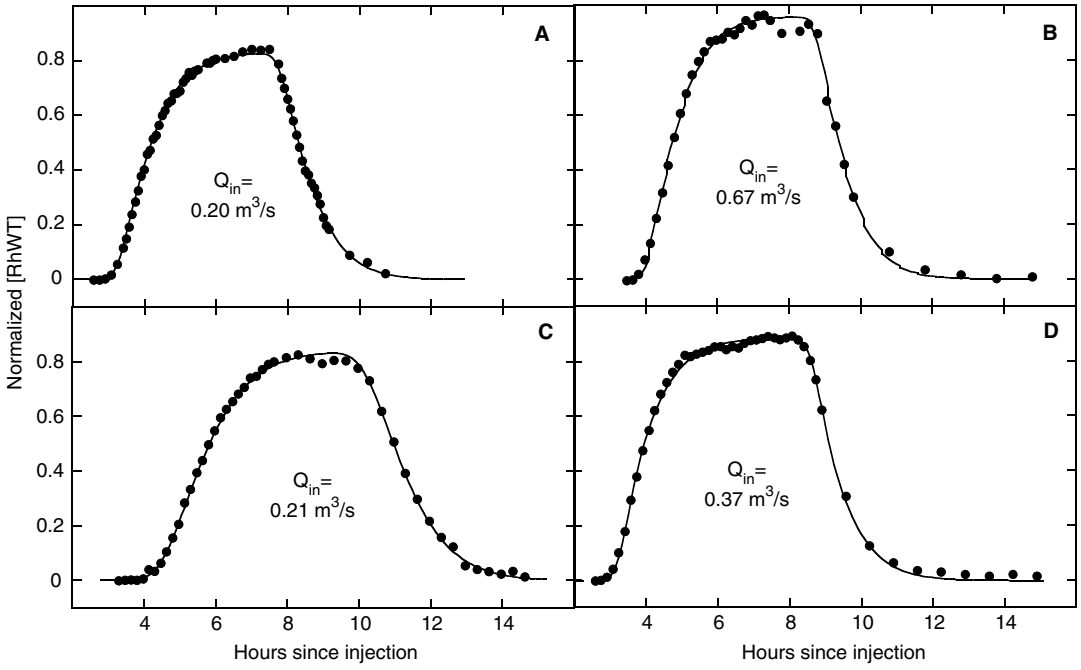

Figure 7 Normalized breakthrough curves for injections along the upper stretch (starting at Km 0.00). Circles are observations, solid lines are best fits with the transient storage model OTIS, as determined with PEST, for the entire data set. (A) 9/4/03; (B) 5/19/04; (C) 7/22/04; (D) 9/2/04.

discharge was relatively low (Fig. 8 and Table 3). Dal numbers for these tests were 0.5—7, and hydrologic exchange parameters were, once again, consistent with earlier studies. In an effort to achieve a better fit to the lower stretch BTCs, we used STAMMT-L (Haggerty and Reeves, 2002), a model allowing a non-exponential distribution of residence times. Results obtained with STAMMT-L were not distinguishable from results obtained with OTIS, and are therefore are not displayed.

On the upper stretch, the lateral inflow length consistently decreases with decreasing discharge, from L_I = 27 km at 0.67 m^3/s to L_I = 7.7 km at 0.20 m^3/s (Fig. 9A). The storage

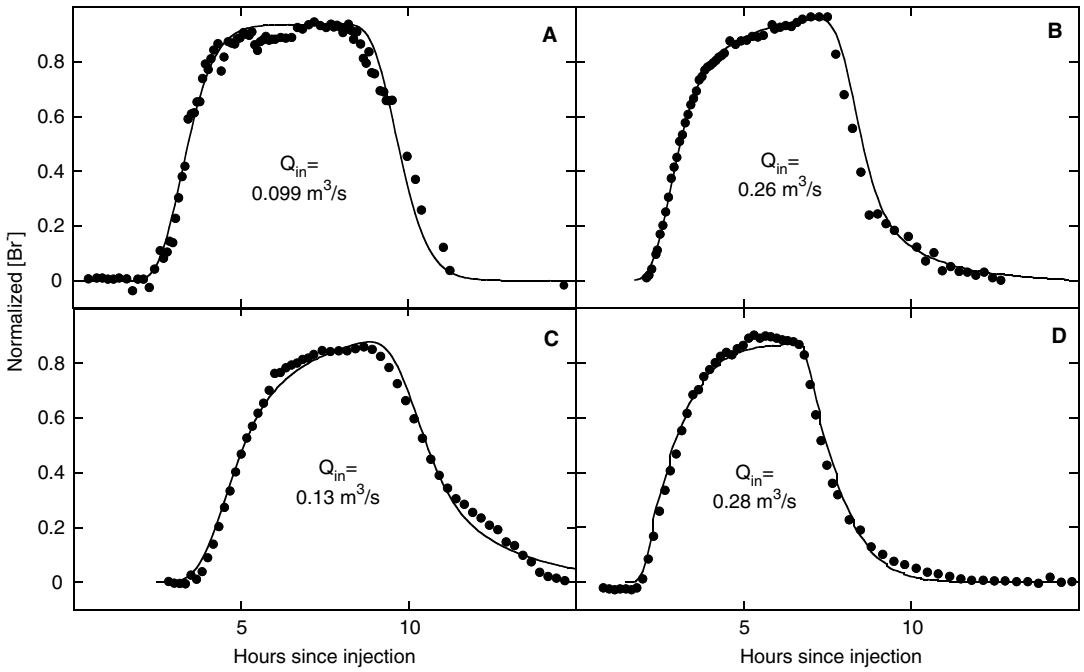

Figure 8 Normalized breakthrough curves for injections along the lower stretch (starting at Km 7.67). Circles are observations, solid lines are best fits with the transient storage model OTIS, as determined with PEST, for the entire data set. (A) 8/26/03, at Km 8.20. (B) 6/15/04, at Km 8.44. (C) 7/20/04, at Km 8.32. (D) 8/31/04, at Km 8.44.

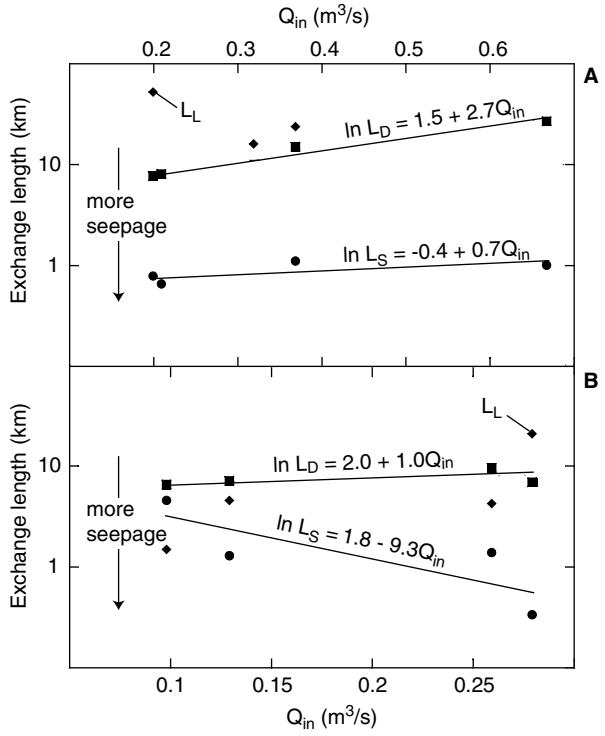

Figure 9 Seepage lengths plotted as a function of channel discharge. Length scales are defined by Eqs. (4)—(6) and discussed in the text. Lateral inflow length (L_I = squares), storage exchange length (L_S = circles), loss lengths (L_L = diamonds). (A) Injections from Km 0. L_S and L_D corresponding to Dal = 204 are not included. (B) Injections from Km 7.67.

exchange length (L_S) also decreases with decreasing discharge, but the slope of the trend is lower. Other model parameters (D, A, A_s, and α) showed no clear trends with discharge (Table 2). The upper stretch generally showed no change in net discharge during these tests, so the loss lengths would be essentially infinite. Along the lower stretch, the inflow length also decreased with decreasing streamflow (Fig. 9B). However, unlike the other length scales discussed here, the storage exchange length (L_S) increased with decreasing discharge, indicating a reduction in this exchange flux (normalized to channel discharge). Channel discharge decreased along the lower stretch during all of the tests, yielding loss lengths of L_L = 1.5—21 km.

Discussion

The Pajaro River lost 0.2—0.4 m^3/s of channel discharge over a 11.42 km reach, equivalent to a loss per unit stream length of 0.2—0.4 cm^2/s. There are several indications that this channel loss results from streambed seepage. First, there are no consistent changes in $\delta^{18}O$ and δ^2H of Pajaro River water from the top to the bottom of the experimental reach (Fig. 6), as would be expected if there were large evaporative losses. Given typical channel losses relative to discharge at Km 0.00, and appropriate isotopic enrichment factors (Gat, 1996), we would expect to see increases of 1.4‰ and 23‰ for $\delta^{18}O$ and δ^2H, respectively, along the reach if half the loss in discharge were to result from evaporation. Given typical analytical errors of ±0.13‰ for $\delta^{18}O$ and ±0.50‰ for δ^2H, evaporation can account for less than 3% of observed channel loss. Reference evapotranspiration rates compiled from nearby CIMIS stations (10—15 cm/month) were equivalent to evapotranspiration losses in

the experimental reach no greater than 5–10% of net loss. We also compared channel loss during day and night and found ⩽5% difference, even during the warmest part of the year. Collectively, these observations demonstrate that little channel loss in the experimental reach results from evapotranspiration.

In addition, Br was detected in piezometer samples taken from depths of 0.5–1.0 m below the top of the streambed along the lower stretch soon after NaBr injections, consistent with downward seepage rates of 0.4–2 m/day. These seepage rates, when multiplied by typical stream widths, yield channel losses that are consistent with differential discharge data, and with head gradients in adjacent piezometers (Fig. 5). Finally, we note that channel losses occur most rapidly near the bottom of the experimental reach, after the Pajaro River crosses the San Andreas Fault and where the Pajaro Valley abruptly widens (Fig. 2) and the alluvial aquifer below the streambed becomes better developed. This observation is consistent with an increase in the rate at which the Pajaro River recharges underlying aquifers.

If the Pajaro River loses water to underlying aquifers at 0.2–0.4 m^3/s throughout the water year, this would result in annual recharge of $6–13 \times 10^6$ m^3, equivalent to ~20–40% of current sustainable yield for the Pajaro Valley (PVWMA, 2001). It will be difficult to quantify the extent of channel loss during periods of higher flow in the Pajaro River using differential discharge techniques because there are additional inputs to the stream during and soon after precipitation events, and normal errors in discharge measurements at higher flows may be considerably larger than the change in channel discharge along the reach. We also note that the lower part of the experimental reach, where the greatest rates of channel loss occur (Fig. 4), typically goes dry towards the end of each water year. Greater aquifer recharge may be possible if flow were maintained through this part of the channel throughout the driest part of the year, preventing the formation of an unsaturated zone below the streambed.

In addition to losing a large fraction of water from the channel along the experimental reach, modeling of tracer test results suggests that there are simultaneous exchange fluxes with storage zones in the Pajaro River system. Within the upper stretch, the flux associated with lateral inflow of unlabeled water is about ten times lower than that associated with storage exchange ($L_I \sim 10 \times L_S$), and both of these fluxes are greater than net channel loss (Fig. 9A). The rate of inflow increases as discharge decreases, whereas the storage exchange flux remains roughly constant with changing discharge. The lower stretch experiences inflow and storage exchange fluxes comparable to those in the upper stretch (Fig. 9B). Once again, inflow increases with decreasing discharge; however, the storage exchange fluxes decrease with decreasing discharge. Channel loss fluxes in the lower stretch are intermediate in magnitude between storage exchange fluxes and inflow, with the former being the largest. Thus even a strongly losing reach of a stream can experience relatively large storage exchange fluxes, probably including exchange with the hyporheic zone.

This last result may seem counterintuitive at first, but it can be explained if one considers the scales and locations at which seepage fluxes may occur. First, storage exchange may include pools, back eddies, and other surface features. However, even if exchange occurs with storage zones in the streambed, this can accompany net seepage loss within the same reach under the right conditions. Stream loss to an underlying aquifer requires that there be an appropriate head gradient (head decreases downward below the bottom of the stream) and that there be a good hydrogeologic connection between the stream and aquifer. Geologic heterogeneity will leave some parts of a channel better connected to underlying aquifers than others, because of differences in hydraulic conductivity under saturated conditions or due to patchy formation of an unsaturated zone below the streambed. Given appropriate head gradients, areas having a good connection with underlying aquifers may experience greater net channel loss, whereas more poorly-connected areas may experience greater storage exchange. There could also be seepage loss through the center of the channel, and local storage exchange along the stream banks on the side of the channel. If the connection between streams and aquifers depends on the distribution of unsaturated zones, these connections may vary in distribution throughout the water year and over longer time periods. In addition, flow paths of water entering the streambed from above may bifurcate (Harvey and Bencala, 1993), with some fraction of this water following paths that return to the stream channel.

Finite-length tracer tests are incapable of distinguishing between ''true'' ground water (having never been in the stream channel) and water that entered the streambed but flows in the shallow subsurface for a time or distance that is too long to be measured. Both of these flows are represented in Eq. (2) as $q_{L,in}$. However, it seems unlikely that the exchange fluxes quantified along the experimental reach of the Pajaro River include large quantities of basin ground water. Shallow ground water samples from aquifers adjacent to the Pajaro River are isotopically distinct from stream water, being depleted in both ^{18}O and ^{2}H (Fig. 6). If a large fraction of $q_{L,in}$ were to comprise isotopically depleted ground water, we would expect to see a decrease in $\delta^{18}O$ and $\delta^{2}H$ of stream water from Km 0.0 to Km 11.42. Similarly, if storage exchange fluxes were to occur with water that was isotopically distinct we would expect to see a change in the $\delta^{18}O$ and $\delta^{2}H$ of channel water. Within the lower part of the experimental reach, where net channel losses are greatest, it is not surprising that ground water input appears to be negligible. An important implication of this interpretation is that lateral inflow may be primarily composed of hyporheic flow that takes a long time and/or follows long flow paths relative to the length and time scales of tracer experiments.

We expected that relative storage exchange fluxes might increase with decreasing channel discharge due to the increasing downstream variation in stream gradients at lower flows (Harvey and Bencala, 1993; Kasahara and Wondzell, 2003; Wondzell and Swanson, 1996). There is a positive correlation between lateral inflow length and channel discharge along both upper and lower stretches (Fig. 9). On the other hand, storage exchange lengths decreased with decreasing discharge along the upper stretch, but increased with decreasing discharge along the lower stretch. The reduction in storage exchange at low discharge along the lower stretch may result from the high rate of channel loss. Increasingly negative head gradients along the lower stretch

as the water year progresses (Fig. 5) may result in a greater fraction of the water that enters the streambed either not returning to the main channel, or returning on a longer length or time scale. This is consistent with the increase in storage exchange length and a decrease in inflow and channel loss lengths as discharge decreases along the lower stretch (Fig. 9B).

We found high lateral inflow and exchange fluxes during the 8/31/04 tracer experiment (Fig. 9B), when channel loss was insignificant relative to earlier in the year. One explanation for these results is that an unsaturated zone developed under the streambed where this test was run, prior to the abrupt upstream release of water to the channel in August 2004 (Fig. 3). This section of the stream channel often goes dry late in the water year and by the time of the late-season release, discharge had nearly ended at the Km 11.42 gauging station. The presence of an unsaturated zone under much of the lower stretch would greatly slow the movement of water from the stream into underlying aquifers (e.g., Constantz and Thomas, 1996), but it would have little influence on exchange fluxes involving the streambed. This explanation is consistent with the earlier interpretation that much of lateral inflow is hyporheic flow that has followed a long path, as opposed to true ground water, because there would be little opportunity for ground water to flow into the stream channel if head levels in the aquifer were low and there was an unsaturated zone separating the stream from the aquifer. This explanation is also consistent with a lack of measurable channel loss along the lower reach during this test, and the resumption in channel loss several weeks later, perhaps when the region below the channel along this stretch became resaturated (Fig. 3). A tracer test run on the upper stretch a few days after that on the lower stretch did not yield anomalously high inflow or exchange fluxes (Fig. 9A), but this part of the experimental reach remains wet throughout the water year (Fig. 3), so it would have been more difficult for an unsaturated zone to develop below the channel.

Conclusions

The Pajaro River consistently loses 0.2–0.4 m^3/s of discharge along an 11.42-km experimental reach late in the water year, when flows are $\leqslant$4.5 m^3/s. Channel loss occurs throughout the experimental reach, but is greatest in magnitude near the bottom of the reach. Water isotopic data and other observations suggest that channel loss is most likely a result of streambed seepage. If it occurs throughout the year, channel loss of this short stream reach could contribute $6–13 \times 10^6$ m^3 of annual recharge to underlying aquifers, ~20–40% of current sustainable basin yield. Thus in the Pajaro Valley and in similar watersheds, quantification of streamed seepage is necessary before basin-wide hydrologic budgets can be determined, and maintenance of discharge in losing reaches might help to maximize aquifer recharge and limit overdraft.

Channel loss in the Pajaro River occurs at the same time as significant storage exchange fluxes and inflow of tracer-free water. The former are associated with the movement of water between the main channel and in-channel or off-channel storage zones, whereas the latter are associated with the inflow to the channel of ground water or hyporheic water that has followed a spatially- or temporally-long flow path. Within upper and lower stretches of the experimental reach, exchange fluxes are about an order of magnitude greater than inflow. Along both upper and lower stretches of the experimental reach, inflow tends to increase as channel discharge decreases; however, with decreasing discharge, storage exchange fluxes increase along the upper stretch but decrease along the lower stretch. Within the lower stretch of the experimental reach, the magnitude of channel loss is greater than lateral inflow, but less than the exchange flux.

We conclude that long-scale hyporheic exchange may occur in losing reaches of some streams, and perhaps in non-losing stream systems as well. Investigators should look for evidence of this in addition to the relatively short-scale exchange commonly measured using the TSM approach. It appears possible for a stream to exchange water between the channel and adjacent storage zones at the same time as it loses water, perhaps because these processes occur within distinct parts of the stream channel. Our study demonstrates that a thorough hydrologic balance obtained by repeated direct measurements of stream discharge, in combination with a TSM approach (Harvey and Wagner, 2000), can constrain seepage fluxes better than either method on its own. Finally, this study suggests that the TSM approach can be used to obtain meaningful stretch-specific hydrologic parameters within a strongly-losing stream.

Acknowledgements

This work was supported by the Committee on Research (UCSC), the STEPS Institute (UCSC), Center for Agroecology and Sustainable Food Systems, the United States Department of Agriculture (Projects # 2003-35102-13531 and 2002-34424-11762), and the National Science Foundation Graduate Fellowship program. In addition, the authors acknowledge field assistance provided by Gerhardt Epke, Remy Nelson, Emily Underwood, Laura Roll, Randy Goetz, Nicole Alkov, Mike Hutnak, Claire Phillips, Ari Hollingsworth, Jean Waldbieser, Kena Fox-Dobbs, Carissa Carter, Pete Adams, Ty Kennedy-Bowdoin, Andy Shriver, Bowin Jenkins-Warrick, Robert Sigler, Heather McCarren, Iris DeSerio, Sora Kim, Heather McCarren, Greg Stemler, and Kevin McCoy. Roy Haggerty kindly provided an updated version of the STAMMT-L model for surface water–ground water exchange with non-exponential residence time distributions. We thank Randy Hanson and Larry Freeman (US Geological Survey) and Jonathan Lear (Pajaro Valley Water Management Agency) for their guidance, encouragement, and assistance. Thoughtful reviews by Michael Gooseff, Ken Bencala, Marissa Cox, and two anonymous reviewers greatly improved this paper.

References

Bahr, J.M., Rubin, J., 1987. Direct comparison of kinetic and local equilibrium formulations for solute transport affected by surface reactions. Water Resources Research 23 (3), 438–452.

Bencala, K.E., 1983. Simulation of solute transport in a mountain pool-and-riffle stream with a kinetic mass transfer model for sorption. Water Resources Research 19 (3), 732–738.

Bencala, K.E., Kennedy, V.C., Zellweger, G.W., Jackman, A.P., Avanzino, R.J., 1984. Interactions of solutes and streambed sediment. 1. An experimental analysis of cation and anion transport in a mountain stream. Water Resources Research 20 (12), 989–1000.

Bencala, K.E., McKnight, D.M., Zellweger, G.W., 1990. Characterization of transport in an acidic and metal-rich mountain stream based on a lithium tracer injection and simulations of transient storage. Water Resources Research 26 (5), 989–1000.

Bencala, K.E., Walters, R.A., 1983. Simulation of solute transport in a mountain pool-and-riffle stream: a transient storage model. Water Resources Research 19 (3), 718–724.

Choi, J., Harvey, J.W., Conklin, M.H., 2000. Characterizing multiple timescales of stream and storage zone interaction that affect solute fate and transport in streams. Water Resources Research 36 (6), 1511–1518.

Constantz, J., Thomas, C.L., 1996. The use of streambed temperature profiles to estimate the depth, duration, and rate of percolation beneath arroyos. Water Resources Research 32 (12), 3597–3602.

Criss, R.E., Davidson, M.L., 1996. Isotopic imaging of surface water/groundwater interactions, Sacramento Valley, California. Journal of Hydrology 178, 205–222.

D'Angelo, D.J., Webster, J.R., Gregory, S.V., Meyer, J.L., 1993. Transient storage in Appalachian and Cascade Mountain streams as related to hydraulic characteristics. Journal of the North American Benthological Society 12 (3), 223–235.

Doherty, J., 2004. PEST: model-independent parameter estimation. Watermark Numerical Computing.

Fernald Jr., A.G., Wigington, P.J., Landers, D.H., 2001. Transient storage and hyporheic flow along the Williamette River, Oregon: field measurements and model estimates. Water Resources Research 37 (6), 1681–1694.

Gat, J.R., 1996. Oxygen and hydrogen isotopes in the hydrologic cycle. Annual Reviews of Earth and Planetary Science 24, 225–262.

Gooseff, M.N., Bencala, K.E., Scott, D.T., Runkel, R.L., McKnight, D.M., 2005. Sensitivity analysis of conservative and reactive stream transient storage models applied to field data from multiple-reach experiments. Advances in Water Research 28 (5), 479–492.

Gooseff, M.N., McKnight, D.M., Runkel, R.L., Vaughn, B.H., 2003a. Determining long time-scale hyporheic zone flow paths in Antarctic streams. Hydrological Processes 17 (9), 1691–1710.

Gooseff, M.N., Wondzell, S.M., Haggerty, R., Anderson, J.K., 2003b. Comparing transient storage modeling and residence time distribution (RTD) analysis in geomorphically varied reaches in the Lookout Creek basin, Oregon, USA. Advances in Water Research 26 (9), 925–937.

Greene, H.G., 1990. Regional tectonics and structural evolution of the Monterey Bay Region, Central California. In: Garrison, R.E., Greene, H.G., Hicks, K.R., Weber, G.E., Wright, T.L. (Eds.), Geology and Tectonics of the Central California Coast Region San Francisco to Monterey. American Association of Petroleum Geologists, Bakersfield, CA, p. 314.

Grimm, N.B., Fisher, S.G., 1984. Exchange between interstitial and surface water: implications for stream metabolism and nutrient cycling. Hydrobiologia 111 (3), 219–228.

Haggerty, R., Reeves, P., 2002. STAMMT-L Version 1.0 User's Manual. Sandia National Laboratories [ERMS #520308], pp. 1–76.

Haggerty, R., Wondzell, S.M., Johnson, M.A., 2002. Power-law residence time distribution in the hyporheic zone of a 2nd-order mountain stream. Geophysical Research Letters 29 (13), 1–4.

Hanson, R.T., 2003. Geohydrologic Framework of Recharge and Seawater Intrusion in the Pajaro Valley, Santa Cruz and Monterey Counties, California. USGS Water-Resources Investigations Report 03-4096.

Harvey, J.W., Bencala, K.E., 1993. The effect of streambed topography on surface–subsurface water exchange in mountain catchments. Water Resources Research 29 (1), 89–98.

Harvey, J.W., Fuller, C.C., 1998. Effect of enhanced manganese oxidation in the hyporheic zone on basin-scale geochemical mass balance. Water Resources Research 34 (4), 623–636.

Harvey, J.W., Wagner, B.J., 2000. Quantifying hydrologic interactions between streams and their subsurface hyporheic zones. In: Streams and Ground Waters. Academic Press, San Diego, CA, pp. 3–44.

Harvey, J.W., Wagner, B.J., Bencala, K.E., 1996. Evaluating the reliability of the stream tracer approach to characterize stream-subsurface water exchange. Water Resources Research 32 (8), 2441–2451.

Hill, A.R., Labadia, C.F., Sanmugadas, K., 1998. Hyporheic zone hydrology and nitrogen dynamics in relation to the streambed topography of a N-rich stream. Biogeochemistry 42 (3), 285–310.

Izbicki, J.A., Stamos, C.L., Nishikawa, T., Martin, P., 2004. Comparison of ground-water flow model particle-tracking results and isotopic data in the Mojave River ground-water basin, southern California, USA. Journal of Hydrology 292, 30–47.

Jones, D.R., Jung, R.F., 1990. Analytical problems arising from the use of bromide and Rhodamine-WT as co-tracers in streams. Water Research 24 (1), 125–128.

Jones, J.B., Mulholland, P.J. (Eds.), 2000. Streams and Ground Waters. Aquatic Ecology Series. Academic Press, San Diego, CA, p. 425.

Kasahara, T., Wondzell, S.M., 2003. Geomorphic controls on hyporheic exchange flow in mountain streams. Water Resources Research 39 (1), 1005. doi:10.1029/2002WR001386.

Kendall, C., Coplen, T.B., 2001. Distribution of oxygen-18 and deuterium in river waters across the United States. Hydrological Processes 15 (7), 1363–1393.

Levy, B.S., Chambers, R.M., 1987. Bromide as a conservative tracer for soil–water studies. Hydrological Processes 1 (4), 385–389.

Malard, F., Tockner, K., Dole-Olivier, M.-J., Ward, J.V., 2002. A landscape perspective of surface–subsurface hydrological exchanges in river corridors. Freshwater Biology 47 (4), 621–640.

McKnight, D.M., Hornberger, G.M., Bencala, K.E., Boyer, E.W., 2002. In-stream sorption of fulvic acid in an acidic stream: a stream-scale transport experiment. Water Resources Research 38 (1), 1–12.

Muir, K.S., 1972. Geology and Ground Water of the Pajaro Valley Area Santa Cruz and Monterey Counties, California. USGS Open-File Report 73-199, pp. 1–80.

Muir, K.S., 1977. Initial Assessment of the Ground-Water Resources in the Monterey Bay Region, California. USGS Water Resources Investigation 77-46. pp. 1–33.

Packman, A.I., Brooks, N.H., 2001. Hyporheic exchange of solutes and colloids with moving bed forms. Water Resources Research 37 (10), 2591–2605.

PVWMA, 2001. Pajaro Valley Water Management Agency State of the Basin Report.

Rains, M.C., Mount, J.F., 2002. Origin of shallow ground water in an alluvial aquifer as determined by isotopic and chemical procedures. Ground Water 40 (5), 552–563.

Rantz, S.E., 1982. Measurement and computation of streamflow. US Geological Survey Water-Supply Paper 2175, 284p.

Ruehl, C., Fisher, A.T., Los Huertos, M., Wankel, S.D., Wheat, C.G., Kendall, C., Hatch, C.E., Shennan, C., 2006. Nitrate dynamics within the Pajaro River, a nutrient-rich, losing stream. Journal of the North American Benthological Society (submitted for publication).

Runkel, R.L., 1998. One-dimensional transport with inflow and storage (OTIS): a solute transport model for streams and rivers. US Geological Survey Water-Resources Investigation Report 98-4018, pp. 1–73.

Runkel, R.L., McKnight, D.M., Andrews, E.D., 1998. Analysis of transient storage subject to unsteady flow: diel flow variation in an Antarctic stream. Journal of the North American Benthological Society 17 (2), 143–154.

Sauer, V.B., Meyer, R.W., 1992. Determination of error in individual discharge measurements. US Geological Survey Open-File Report, pp. 92–144.

Shiau, B.J., Sabatini, D.A., Harwell, J.H., 1993. Influence of rhodamine WT properties on sorption and transport in subsurface media. Ground Water 31 (6), 913–920.

Smart, P.L., Laidlaw, I.S., 1977. An evaluation of some fluorescent dyes for water tracing. Water Resources Research 13 (1), 15–33.

Storey, R.G., Howard, K.W.F., Williams, D.D., 2003. Factors controlling riffle-scale hyporheic exchange flows and their seasonal changes in a gaining stream: a three-dimensional groundwater flow model. Water Resources Research 39 (2), 1034. doi:10.1029/2002WR001367.

Sutton, D.J., Kabala, Z.J., Francisco, A., Vasudevan, D., 2001. Limitations and potential of commercially available rhodamine WT as a groundwater tracer. Water Resources Research 37 (6), 1641–1656.

Triska, F.J., Kennedy, V.C., Avanzino, R.J., Zellweger, G.W., Bencala, K.E., 1989. Retention and transport of nutrients in a third-order stream in northwestern California: hyporheic processes. Ecology 70 (6), 1893–1905.

Valett, H.M., Morrice, J.A., Dahm, C.N., Campana, M.E., 1996. Parent lithology, surface–groundwater exchange, and nitrate retention in headwater streams. Limnology and Oceanography 41 (2), 333–345.

Vecchia, A.V., Cooley, R.L., 1987. Simultaneous confidence and prediction intervals for nonlinear regression models with application to a groundwater flow model. Water Resources Research 23 (7), 1237–1250.

Wagner, B.J., Harvey, J.W., 1997. Experimental design for estimating parameters of rate-limited mass transfer: analysis of stream tracer studies. Water Resources Research 33 (7), 1731–1741.

Williams, D.D., Haynes, H.B.N., 1974. The occurrence of benthods deep in the substratum of a stream. Freshwater Biology 22, 189–208.

Wilson, J.F., Jr., Cobb, E.D., Kilpatrick, F.A., 1986. Fluorometric procedures for dye tracing. US Geological Survey Techniques of Water-Resource Investigations 03-A12, pp. 1–34.

Winter, T.C., Harvey, J.W., Franke, O.L., Alley, W.M., 1998. Groundwater and surface water, a single resource. US Geological Survey Water Related Circular 1139.

Woessner, W.W., 2000. Stream and fluvial plain ground water interactions: rescaling hydrogeologic thought. Ground Water 38 (3), 423–429.

Wondzell, S.M., Swanson, F.J., 1996. Seasonal and storm dynamics of the hyporheic zone of a 4th-order mountain stream. 2. Nitrogen cycling. Journal of the North American Benthological Society 15 (1), 20–34.

Worman, A., Packman, A.I., Johansson, H., Jonsson, K., 2002. Effect of flow-induced exchange in hyporheic zones on longitudinal transport of solutes in streams and rivers. Water Resources Research 38 (1), 1001. doi:10.1029/2001WR000769.

Zaramella, M., Packman, A., Marion, A., 2003. Application of the transient storage model to analyze advective hyporheic exchange with deep and shallow sediment beds. Water Resources Research 39 (7).